ATLAS Diamond Beam Conditions Monitor

Irena Dolenc[*a], **V. Cindro**[a], **D. Dobos,**[d], **H. Frais-Kölbl**[b], **A. Gorišek**[a], **E. Griesmayer**[b], **H. Kagan**[c], **B. Maček**[a], **I. Mandić**[a], **M. Mikuž**[a], **M. Niegl**[b], **H. Pernegger**[d], **S. Smith**[c], **D. Tardif**[e], **W. Trischuk**[e], **P. Weilhammer**[e], **M. Zavrtanik**[a]

[a] *Jožef Stefan Institute, Ljubljana, Slovenia*

[b] *University of Applied Science, Wiener Neustadt, Austria*

[c] *Ohio State University, Columbus, USA*

[d] *CERN, Geneva, Switzerland*

[e] *University of Toronto, Toronto, Canada*

E-mail: irena.dolenc@ijs.si

The primary goal of the ATLAS Beam Conditions Monitor (BCM) system is to detect early signs of beam instabilities and protect the ATLAS detector against damaging beam losses by initiating the beam abort. BCM will monitor instantaneous particle rates close to the interaction point on a bunch-by-bunch basis. Additionally, it will provide coarse luminosity information.

The ATLAS BCM consists of two stations with four detector modules each. Each module includes two diamond pad sensors read out in parallel. Detector stations are placed symmetrically around the interaction point with diamond sensors at z=184 cm and r=5.5 cm. Using fast electronics ($\sim$2 ns shaping time) these detectors will measure time-of-flight and pulse amplitude in order to distinguish between normal collisions and background events due to natural or accidental beam losses.

The digitisation of BCM analogue signals is based on the NINO amplifier-discriminator chip, which encodes the analogue signal amplitude as time-over-threshold information.

The final design of BCM system together with a summary of results of analogue and digital signal studies is described. An estimate of overall BCM system performance as expected in ATLAS is also given.

---

[*]Speaker

1. Introduction

The LHC will circulate 2808 proton bunches per colliding beam with each bunch consisting of 1.1×10^{11} protons at 7 TeV energy. The total energy stored in one LHC beam will be more than two orders of magnitude above the maximum beam energy stored in previous high energy colliders like Tevatron or HERA. If there is a failure in an element of the accelerator the resulting beam losses could cause substantial damage to the experiments. The LHC experiments have decided to develop their own protection systems in addition to those provided by the accelerator. The aim of the Beam Conditions Monitor (BCM) system in ATLAS is to monitor beam conditions close to the interaction point inside the ATLAS Inner Detector. It is designed to detect early signs of beam instabilities and initiate a beam abort if needed. In addition, it will also provide a coarse luminosity measurement as complementary information to LUCID, the ATLAS main luminosity monitor. Accidental beam losses can result in beam scraping the beam pipe or collimator (TAS) close to the entrance to the ATLAS cavern which produces a shower of particles upstream the beam (see figure 1). Natural losses can also occur. These include beam halo protons interacting with the TAS collimator and beam-gas interactions, both similarly resulting in showers of particles upstream the beam. The principle of operation is shown in figure 2. Two BCM detector stations are placed symmetrically around the interaction point at $z_{bcm} = \pm 1.84$ m. Collisions at the interaction point occurring every proton bunch crossing give signals in both detector stations simultaneously (*in–time hits*). On the other hand, shower particles originating from $|z| > |z_{bcm}|$ hit the nearest station at a time $\delta t = 2z_{bcm}/c \sim 12.3$ ns before the station on the other side (*out-of-time hits*), which corresponds to about half of the time difference between two consecutive bunch crossings. Thus, the *out-of-time* hits are used to identify the the background events while the *in-time* hits are used to monitor the luminosity on the bunch-by-bunch basis.
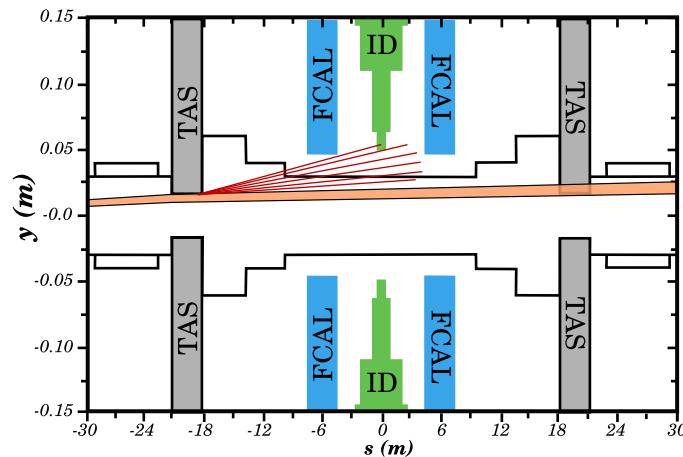

Figure 1: An example of a simulated beam accident in ATLAS[1] where proton beam hits the TAS collimators. The horizontal scale corresponds to the whole ATLAS cavern, while the vertical scale is a zoom around the beam pipe, therefore only the Inner Detector (ID) and Forward Calorimeter (FCAL) are visible. The orange area represents the range of beam directions dangerous for the Inner Detector. Red lines denote shower particles.
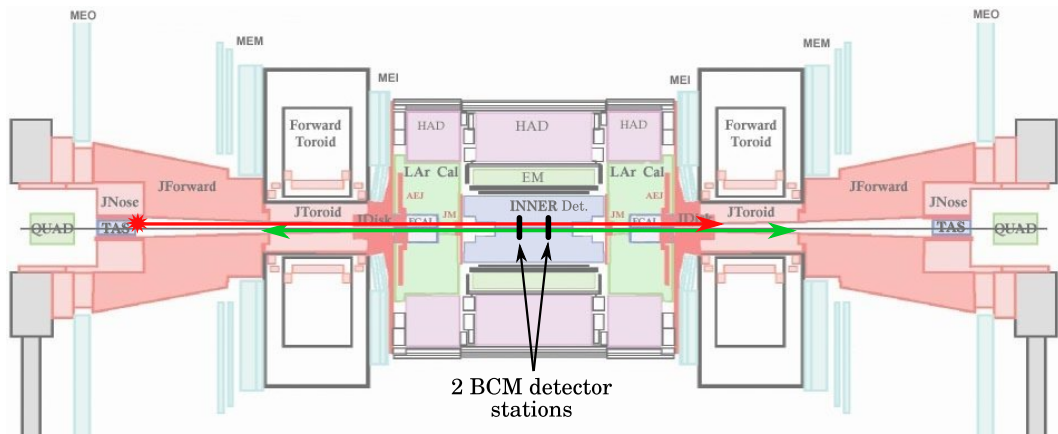
2

Figure 2: ATLAS detector with two BCM detector stations at $\pm z_{bcm}$. Shower particles (red line) reach left stations z_{bcm}/c before interactions at the interaction point occur. Secondary particles from interactions (green line) reach both stations z_{bcm}/c after interactions simultaneously.

2. ATLAS BCM system

There are four BCM detector modules on each side of interaction point, placed symmetrically around the beam beam pipe (figure 3). They are mounted on the ATLAS Pixel detector support structure at 45° towards the beam pipe, with BCM sensors located at r~55 mm corresponding to pseudorapidity of $\eta{\sim}4.2$[1].

The hostile radiation environment and high rate of interactions pose stringent requirements to BCM sensors and electronics. The radiation field at sensor location is expected to amount to about 10^{15} particles per cm^2 and the ionisation dose of $\sim$0.5 MGy in 10 years of ATLAS operation. In order to be able to optimally distinguish between normal collisions and background, BCM detectors should provide signal pulses with rise time of $\sim$1 ns, width of $\sim$3 ns and baseline restoration in less then 10 ns. Furthermore, the BCM system should be sensitive to single minimum ionising particles (MIPs), a requirement for the luminosity assessment.

Polycrystalline chemical vapour deposition (pCVD) diamonds were chosen for the BCM sensor material due to their radiation hardness and fast signals. In addition, diamond sensors exhibit very low leakage current which allows operation at room temperature without cooling. Sensors were developed by RD42 collaboration [2] in cooperation with Element Six Ltd [4] (later transferred to Diamond Detectors Ltd.). They are approximately 500 μm thick with 8$\times$8cm^2 proprietary radiation hard contacts made at Ohio State University. In order to achieve high and narrow signal pulses the sensors are operated close to the charge carrier saturation velocity, at bias voltage of $\pm$1000 V. At 1000 V a typical sensor has a leakage current below 100 pA and a charge collection distance of around 220 μm.

To increase the signal amplitude two diamond sensors acting as a single signal current source are used. The summation is achieved by mounting the two diamonds in a stack ("double decker") configuration where the electrodes of the two diamonds facing each other are shorted at ground potential and connected to the amplifier. The two outer electrodes are connected to the bias voltage

---

[1]The pseudorapidity is defined as $\eta = -\ln(\tan(\Theta/2))$, where Θ is the angle to the beam axis.
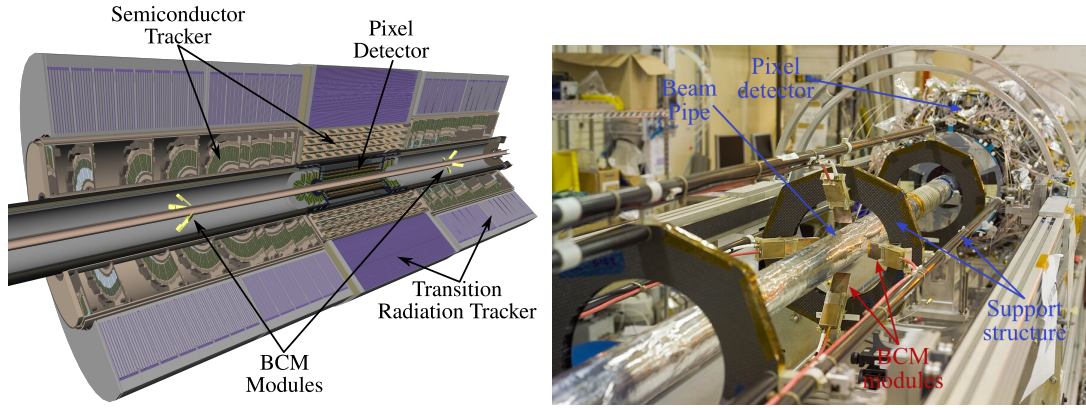
Figure 3: The BCM detector modules in their intended position inside the ATLAS Inner Detector (left), as visualised by the ATLAS event display VP1[3]. Modules are mounted on the Pixel support structure (right).
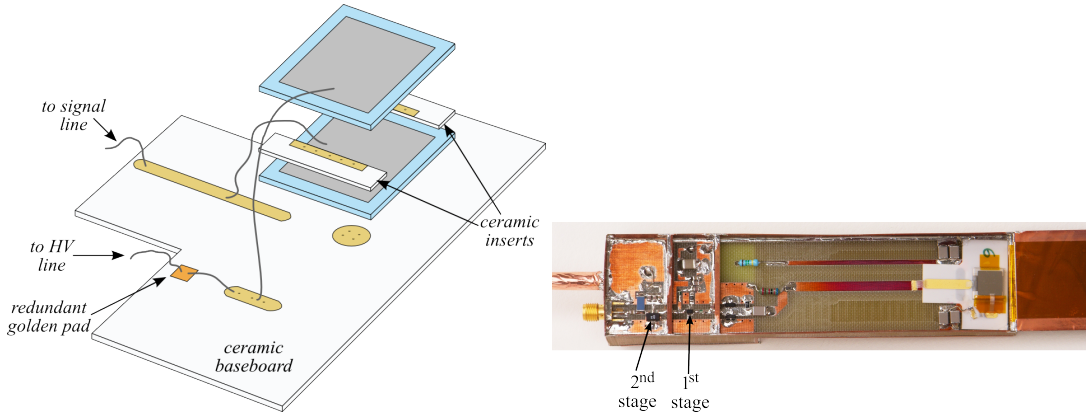

Figure 4: Left: Sketch of the diamond double decker assembly. Right: BCM detector module with the two FE amplifier stages and pCVD diamond sensors.

providing a drift field of $2\,V/\mu m$ in both sensors in the stack. The diamond stack is assembled on a Al_2O_5 ceramic baseboard (figure 4). The high voltage is applied through metal traces on the baseboard to the lower electrode of the lower diamond in the stack and to the pad on the side which is used to bring the high voltage to the upper side of the top plane through wire bonds. Small ceramic distance holders with metal traces are used to conductively glue the two signal electrodes in the middle of the stack together.

 The ceramic assembly is mounted in the detector module where the signal is routed over a $5\,cm$ long transmission line on the printed circuit board to the front-end amplifier (figure 4). In this way the radiation field at the amplifier location is decreased by 30%. The front-end amplifier consists of a two stage current amplifier utilising a $500\,MHz$ Agilent MGA-62563 GaAs MMIC amplifier in the first stage and a $1\,GHz$ Mini Circuit Gali 52 HBT amplifier in the second stage. Each stage provides an amplification of about $20\,dB$ with the first stage exhibiting an excellent noise factor of 0.9dB.

Analogue signals from each BCM detector module are routed through $14\,m$ of coaxial cable to the region behind the ATLAS calorimeter where lower radiation levels are expected (ionisation dose

of ∼10 Gy in 10 years of ATLAS operation). Here, electronics based on the NINO chip [5] is used for digitisation of analogue signals. The NINO ASIC was originally developed by CERN-MIC for time-of-flight measurements of the ALICE RPC detector. Its LVDS output signal exhibits a rise time of ∼1 ns and ∼25 ns jitter. It serves as amplifier and discriminator with time-over-threshold measurement capability. The NINO chip converts an input analogue signal into a digital signal at fixed time after input signal arrival. The charge seen at the input is encoded in terms of time-over-threshold. Thus, the width of the resulting digital output signal is correlated to the amplitude of the input signal.

Each BCM module is connected to a separate custom electronics board with the NINO chip. The board first filters the input signal through a fourth order low-pass filter with a 200 MHz frequency cutoff. This additional filtering was included since studies had shown it to improve the signal-to-noise ratio. After filtering, the signal is split into two parts (high and low amplitude channel) in a ratio of approximately 1:11 to increase the NINO dynamic range. These two signals are then fed into two NINO chip inputs. The resulting two digital signals are further converted into optical signals and transmitted through 70 m of optical fibres to the ATLAS USA15 service cavern. Here, they are converted to PECL electrical signals which are further fed to two FPGA-based data processing units. They are based on the Xilinx ML410 development board featuring the Xilinx Vitrex-4 FPGA chip with 8 RocketIO serial input/output channels that sample the received signals with a frequency of 2.56 GHz. The RAM, present on Xilinx boards, acts like a ring buffer and stores the BCM signal information for about 3×10^6 of the latest LHC bunch crossings.

The BCM system provides different information to several ATLAS and LHC systems through the FPGA. The FPGA processes the input signals in real-time, extracting the signal pulse width and signal arrival time for all low and high amplitude channels of each BCM module. This information is stored as part of the ATLAS DAQ data stream. The BCM system also provides information to the ATLAS Level–1 trigger system, allowing for triggering on topologically interesting events. Additional analysis performed with the FPGA includes determination of *in-time* and *out-of-time* hits, rates and trends for individual modules as well as different logical combinations of signals. In case of beam failure two redundant signals, indicating that beam conditions in the ATLAS Inner Detector have reached an unacceptable level, are sent to the LHC beam abort system which will trigger a beam abort. Alarm and warning signals are sent to the ATLAS Detector control system (DCS) and in more severe cases to the ATLAS hardware interlock system (Detector Safety System - DSS). More sophisticated information (average rates, histograms, etc.) is available to ATLAS and LHC control through DCS channel. In case of beam abort all information stored in the ring buffer of the FPGA board is transferred through DCS for post mortem analysis.

3. Results

3.1 Detector modules

The BCM detector modules were tested with electrons from ^{90}Sr in a laboratory setup and with test beam particles at various stages of their development to optimise the MIP performance in terms of signal-to-noise ratio (SNR). Here the SNR is referred to as the ratio between the most probable (MP) signal amplitude and noise RMS. A short overview of the results is given below, for details see [6, 7, 8, 9].

- Using two diamonds in a double decker configuration gives about two times higher most probable (MP) amplitude compared to a single sensor while the increase of noise RMS is found to be only around 30%.

- Inclining the sensors by an angle of 45° with respect to the incoming ionising particles increases the signal by the geometrical factor of $\sqrt{2}$. Since an average particle track hitting the BCM sensors in ATLAS is expected to be almost parallel to the beam pipe, the BCM sensors are tilted by 45° towards the beam pipe as shown on figure 3.

- Noise was found to be independent on electric filed strengths up to $3\,\mathrm{V}/\mu\mathrm{m}$ and independent on BCM detector module leakage currents up to $0.5\,\mu\mathrm{A}$.

- Simulation showed that the optimal SNR can be achieved with addition of a low-pass filter with frequency cutoff between 200-300 MHz. The SNR was measured to improve by $\sim$15% when the bandwidth at the readout was limited to 200 MHz. With ^{90}Sr electrons as a source of MIPs at normal incidence, typical SNR values of 7.0-7.5 were achieved with final BCM modules for a 200 MHz bandwidth limit set at the readout.

- With test beam MIPs at 45° incidence rise time of $\sim$1.5 s and FWHM of $\sim$2.8 ns was measured at 200 MHz bandwidth limit. With a 300 MHz bandwidth limit applied at the readout the timing resolution of analogue signals was measured to be better than 400 ps in the threshold range between 0.1 and 2 MP amplitude of MIP signal.

- The analogue signal efficiency for MIP signals was evaluated over the sensor surface using test beam measurements (figure 5). The response was observed to show some non-uniformity at higher thresholds. One possible explanation for this is the grain structure of the pCVD diamond material.

Eleven modules have undergone final thermo-mechanical tests and the best eight have been installed on the ATLAS Pixel detector support structure since the end of 2006 and were lowered to the ATLAS cavern in June 2008.
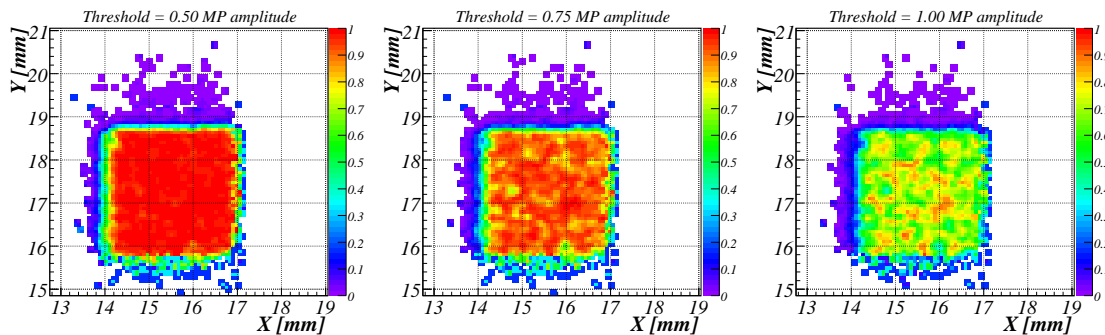

Figure 5: Efficiency of analogue signals scanned over part of diamond double decker area in steps of 0.1 mm. At each step, the efficiency was calculated as the fraction of MIP tracks in $0.2{\times}0.2\,\mathrm{mm}^2$ with a signal amplitude higher than a threshold value. Threshold value in units of most probable (MP) amplitude is indicated above individual plot.

3.2 NINO digitisation

In 2007 different prototype electronics boards with NINO chip were tested with CERN SPS test beam pions at 45° incidence providing MIP signals. The spare final detector modules and all the final services were used. The measurements presented here were performed on the NINO channel with the higher input signal (high amplitude channel).

The NINO discriminator threshold was varied to evaluate its effect on the efficiency for a pion, traversing the diamond sensors, producing a signal at the NINO output. In the offline analysis the efficiency at a given NINO discriminator threshold was calculated as the fraction of events with NINO signal present in a 20 ns time interval. Measured efficiency curves are shown in figure 6 for different configurations of NINO prototype boards and detector modules connected.

During periods without beam, the noise rate was measured at the output of the NINO board as a function of the NINO threshold for each of the boards with different modules connected to it (see figure 6). According to [10], the noise rate dN/dt in a threshold discriminator readout exhibits the following dependence on the threshold U_{Thr}

$$\ln(dN/dt) \propto \left[-\frac{U_{Thr}^2}{2\sigma^2} \right]. \tag{3.1}$$

The relation is valid if the noise follows the Gaussian distribution with the width σ. The function 3.1 was fitted to the measured noise rate curves to extract the noise RMS σ in units of NINO threshold.

From measured efficiency curves one can extract the median signal as the NINO threshold corresponding to 50% efficiency. Using the median signal values, together with the extracted noise RMS σ, one can calculate the median SNR. This gives a measure for the overall system performance in-
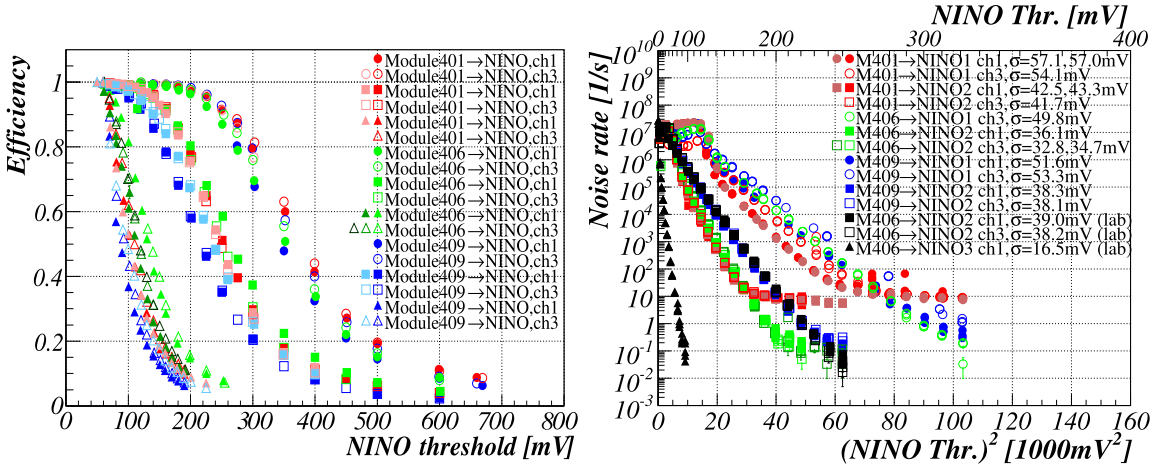

Figure 6: Measured NINO signal efficiency (left) and noise rate (right) dependence on NINO discriminator threshold measured with different prototype NINO boards (different markers) and various BCM detector modules (different colours) connected to them. Open and closed markers correspond to two separate NINO board input channels that connect the signal to two NINO chip input channels through identical routing. Black curves denote the measurements obtained with the laboratory setup, while other curves were obtained during the CERN SPS test beam. Noise RMSs, extracted form the fit to noise rate measurements, are indicated in legend.
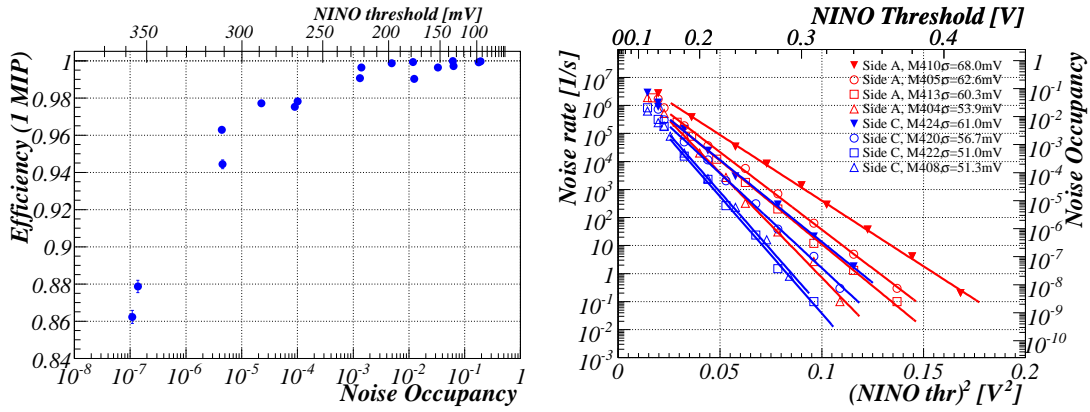
Figure 7: Left: Estimated efficiency for MIP versus noise occupancy (number of fake hits per bunch crossing) as expected for the ATLAS BCM system at the end of readout chain. Right: Noise rate of installed modules as measured at the end of readout chain. The extracted noise RMSs are given in the legend.

cluding both the analogue performance of the BCM detector modules and the digital performance of the NINO board. A median SNR between 6.0 and 8.8 was measured with the prototype NINO boards depending on the board and detector module. The prototype NINO board that showed the best performance in terms of median SNR was chosen for the ATLAS BCM system. However, in order to extend the NINO threshold range to higher values, thus making the system more manageable, an additional amplification (Mini Circuit Gali-52, gain ~3) was added to the final NINO boards.

These test beam measurements were also used for the estimation of the timing resolution of digital signals after the full readout chain. This was found to be better than ~800 ps for NINO threshold settings between ~0.5 and ~1.8 median MIP signal.

The performance of the final NINO boards was examined on a spare final BCM detector module in a laboratory setup. Efficiency and noise rate dependence on NINO discriminator threshold were measured. Electrons from ^{90}Sr, producing non-MIP signals, were used to evaluate the efficiency curve. In order to estimate the noise rates and MIP efficiency of BCM system, which can be expected in ATLAS at the end of the BCM read-out chain (up to the input to FPGA board), the noise rate and efficiency curves as measured with the laboratory setup were scaled by appropriate factors. The factors were determined by comparison of laboratory and test beam results obtained for prototype NINO boards. These factors account for different signal attenuation in the laboratory compared to that in ATLAS, and in case of efficiency also for the non-MIP signals used in laboratory setup. From the resulting efficiency and noise rate curves expected for the BCM system in ATLAS one can estimate for the median signal due to MIPs at 45° incidence to be 575 ± 30 mV and for the noise RMS σ to be around 64 mV giving a median SNR of 9.0 ± 0.5.

The two curves, expected efficiency and noise rate, can be combined in a plot of MIP efficiency versus noise occupancy presented in figure 7. Here, the noise occupancy was calculated as the noise rate in a time interval between two successive LHC bunch crossings (25 ns). From this one can estimate a range of NINO thresholds between 230 mV to 300 mV where the BCM system can be operated with a noise occupancy between 10^{-3} and 10^{-5} and an efficiency between 99% and 96%. This plot, however, gives an estimate for a single module. The exact level of fake hits per

bunch crossing in ATLAS depends on what kind of logical combination of signals from eight BCM modules will be used and could be additionally suppressed by narrowing the time interval beyond bunch crossing time.

The noise rate of installed BCM system, measured just in front of the the signal input into BCM back-end (FPGA), is shown in figure 7. The extracted noise RMS σ were found to be in the range between 50 mV and 70 mV which agrees well with the scaled laboratory measurement with one of the spare BCM detector modules and NINO electronics boards mentioned in previous paragraph.

4. Summary

Tests of the BCM system have shown that adequate performance in terms of SNR and timing can be achieved. It is estimated that for a typical detector module a median MIP SNR of $\sim$9.0 can be expected at the end of ATLAS BCM readout chain up to the input to the FPGA board. Test beam measurements show that timing resolution better than 800 ps for a NINO discriminator threshold range between 0.5 and 1.8 of median MIP signal can be expected.

The full readout chain was operated during the first LHC single beams in September 2008 and is now ready for the first collisions following the LHC repair.

References

[1] D. Bocian, *Accidental beam losses during injection in the interaction region IR1*, LHC Project Note **335**, January 2004

[2] CERN RD-42 Collaboration: *CVD Diamond Radiation Detector Development* (http://rd42.web.cern.ch/RD42/)

[3] T. Kittelmann et al., *The Virtual Point 1 event display for the ATLAS experiment*, CHEP 2009, Prague, Czech Republic, 21-27 Mar 2009

[4] Element Six Ltd, Kings Ride Park, Ascot, Berkshire SL5 8BP, UK

[5] F. Anghinolfi et al., *NINO: an ultra-fast and low-power front-end amplifier and discriminator ASIC for the multi-gap resistive plate chambers*, Nucl. Instr. and Meth. A **553** (2004) 183-187

[6] M. Mikuž et al., *The ATLAS Beam Conditions Monitor*, IEEE Nucl. Sci. Symp. Conf. Rec. 3 (2005) 1360

[7] A. Gorišek et al., *ATLAS diamond Beam Condition Monitor*, Nucl. Instr. and Meth. A **572** (2007) 67-69

[8] W. Trischuk et al., *The ATLAS Beam Conditions Monitor*, JINST, **3** (2008) P02004

[9] I. Dolenc, *Development of Beam conditions monitor for ATLAS experiment*, Ph.D. thesis, University of Ljubljana, 2008

[10] S.O. Rice, *Mathematical analysis of random noise*, Bell System Technical Journal, **23** (1949), 228-332; **24** (1949), 46-156